

Improving Tail-Class Representation with Centroid Contrastive Learning

Anthony Meng Huat Tiong^{1,2} Junnan Li¹ Guosheng Lin² Boyang Li²
 Caiming Xiong¹ Steven C.H. Hoi¹

¹Salesforce Research ²Nanyang Technological University

{anthony.tiong, junnan.li, cxiong, shoi}@salesforce.com {gslin, boyang.li}@ntu.edu.sg

Abstract

In vision domain, large-scale natural datasets typically exhibit long-tailed distribution which has large class imbalance between head and tail classes. This distribution poses difficulty in learning good representations for tail classes. Recent developments have shown good long-tailed model can be learnt by decoupling the training into representation learning and classifier balancing. However, these works pay insufficient consideration on the long-tailed effect on representation learning. In this work, we propose interpolative centroid contrastive learning (ICCL) to improve long-tailed representation learning. ICCL interpolates two images from a class-agnostic sampler and a class-aware sampler, and trains the model such that the representation of the interpolative image can be used to retrieve the centroids for both source classes. We demonstrate the effectiveness of our approach on multiple long-tailed image classification benchmarks. Our result shows a significant accuracy gain of 2.8% on the iNaturalist 2018 dataset with a real-world long-tailed distribution.

1. Introduction

In recent years, deep learning algorithms have achieved impressive results in various computer vision tasks [10, 31]. However, long-tailed recognition remains as one of the major challenges. Different from most human-curated datasets where object classes have a balanced number of samples, the distribution of objects in real-world is a function of Zipf’s law [41] where a large number of tail classes have few samples. Thus, models typically suffer a decrease in accuracy on the tail classes. Since it is resource-intensive to curate more samples for all tail classes, it is imperative to address the challenge of long-tailed recognition.

In the literature of long-tailed recognition, typical approaches address the class imbalance issue by either data re-sampling [2, 13, 42] or loss re-weighting techniques [23,

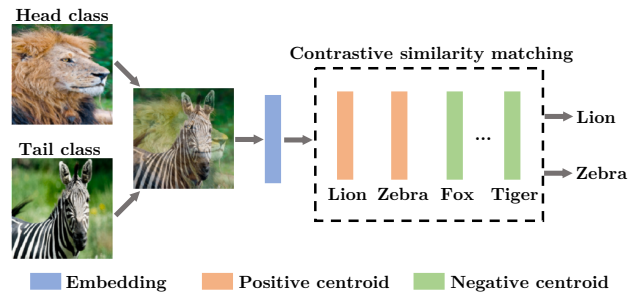


Figure 1: Illustration of interpolative centroid contrastive learning. Given an interpolative sample, we encourage its embedding to have high similarity with its corresponding head-class centroid and tail-class centroid, by contrasting it with the negative centroids.

8, 44, 1, 30]. Re-sampling facilitates the learning of tail classes by shifting the skewed training data distribution towards the tail through undersampling or oversampling. Re-weighting modifies the loss function to encourage larger gradient contribution or decision margin of tail classes.

In order to correctly classify tail-class samples, it is crucial to learn discriminative representations. However, recent developments [1, 22, 59, 9] have discovered that conventional re-sampling and re-weighting methods can lead to a suboptimal long-tailed representation learning. In light of these findings, various approaches proposed to decouple representation learning and classifier balancing [22, 1, 59]. However, most of these works focus on addressing classifier imbalance and pay inadequate attention on the negative effect of long-tailed distribution on representation learning. Thus, an intriguing question remains: can we improve long-tailed representation learning?

We propose interpolative centroid learning (ICCL), a framework to learn more discriminative representations for tail classes. The intuition behind our method is to use the head classes to facilitate representation learning of the tail classes. Inspired by Mixup [57], we create virtual training samples by interpolating two images from two samplers: a class-agnostic sampler which returns all

images with equal probability, and a class-aware sampler which focuses more on tail-class images. The key idea of ICCL is shown in Figure 1. The representation of an interpolative sample should contain information that can be used to retrieve both the head-class centroid and the tail-class centroid. Specifically, we project images into a low-dimensional embedding space, and create class centroids as average embeddings. Given the embedding of the interpolative sample, we query the class centroids with a contrastive similarity matching, and train our model such that the embedding has higher similarities with the correct class centroids.

By injecting class-balanced knowledge in the form of centroids, the proposed interpolative centroid contrastive loss encourages the tail centroids to be positioned discriminatively relative to the head classes. However, the interpolative sample may conflate a head class and a tail class. Thus, we adopt the regular classification loss (top branch in Figure 2) to perform representation learning for head classes, so that the head classes themselves are well positioned. These loss components reinforce one another.

We evaluate the effectiveness of our approach on multiple standard benchmarks of different scale, including CIFAR-LT [1], ImageNet-LT [36] and iNaturalist 2018 [47]. We compare our methods with existing state-of-the-arts including Decouple [22], BBN [59], and Decfound-TDE [45].

We summarise our contribution as follows:

- We introduce interpolative centroid contrastive learning for discriminative long-tailed representation learning. ICCL reduces intra-class variance and increases inter-class variance by optimising the distance between sample embeddings and the class centroids.
- Different from previous findings that suggest class-agnostic training leads to high quality long-tailed representations, ICCL improves tail-class representations by addressing class imbalance with class-aware sample interpolation.
- ICCL achieves significantly high performance on multiple long-tailed recognition benchmarks. Notably, it achieves a substantial accuracy improvement of 2.8% on the large-scale iNaturalist 2018. We also perform ablation study to verify the effectiveness of each proposed component.

2. Related work

Re-sampling. Re-sampling aims to address the imbalance issue from the data level. Two main re-sampling approaches include oversampling and undersampling. Oversampling [2, 3, 15] increases the number of tail-class samples at the risk of overfitting the model, whereas undersampling might reduce the head classes diversity by decreasing

their sample numbers [13, 35]. Class-balanced sampling assigns equal sampling probability for all classes, and then selects their respective images uniformly [42].

Re-weighting. Re-weighting methods modify the loss function algorithmically to improve the learning of tail classes [61, 23, 20, 30, 12, 44]. Cui *et al.* [8] introduced class-balanced loss based on the effective class samples, which improves upon the approaches that assign class weight inversely proportional to their sample number [40, 19, 38]. Another branch of work focuses on improving the decision boundary by enforcing margin between classes [1, 34, 33, 50, 11]. Menon *et al.* [39] proposed logit adjustment to softmax loss that considers the pairwise class relative margin from statistical perspective.

Feature Transfer. Another research direction for long-tailed recognition focuses on transferring the feature representation from head to tail classes [58, 32, 52, 9, 7]. OLTR [36] transfers features of head classes to tail classes using memory centroid features. Rather than just having a centroid for each category, Zhu *et al.* [62] extended OLTR by storing multiple features in both local and global memory bank to address the high intra-class variance issue.

Decoupled Strategy. Several studies have observed that applying re-sampling and re-weighting methods at the beginning of the training process will harm the learning of long-tailed representations [1, 59, 22]. BBN [59] introduces an extra re-balancing branch which focuses on tail classes. The conventional uniform branch and the re-balancing branch are trained simultaneously in a curriculum learning manner. Kang *et al.* [22] discovered that the long-tailed distribution has more negative impact on the classifier than the representation. They proposed a decoupled training approach, where it first performs representation learning without any re-sampling, and then rebalances the classifier in the second stage. Our method follows a similar two-stage training. However, we show that long-tailed representation learning can be further improved by our proposed interpolative centroid contrastive learning even before the classifier rebalancing stage.

It is worth noting that ensemble methods have also been proposed to improve long-tailed classification accuracy [54, 51, 59]. Wang *et al.* [51] reduced the computation complexity of ensemble by only assigning uncertain samples to extra experts dynamically.

Contrastive learning. Recently, contrastive learning approaches have demonstrated strong performance in self-supervised representation learning [4, 16, 5, 14, 53, 56]. Self-supervised contrastive learning projects images into low-dimensional embeddings, and performs similarity matching between images with different augmentations. Two augmented images from the same source image are encouraged to have higher similarity in contrast to others. Prototypical contrastive learning [29] introduces cluster-based

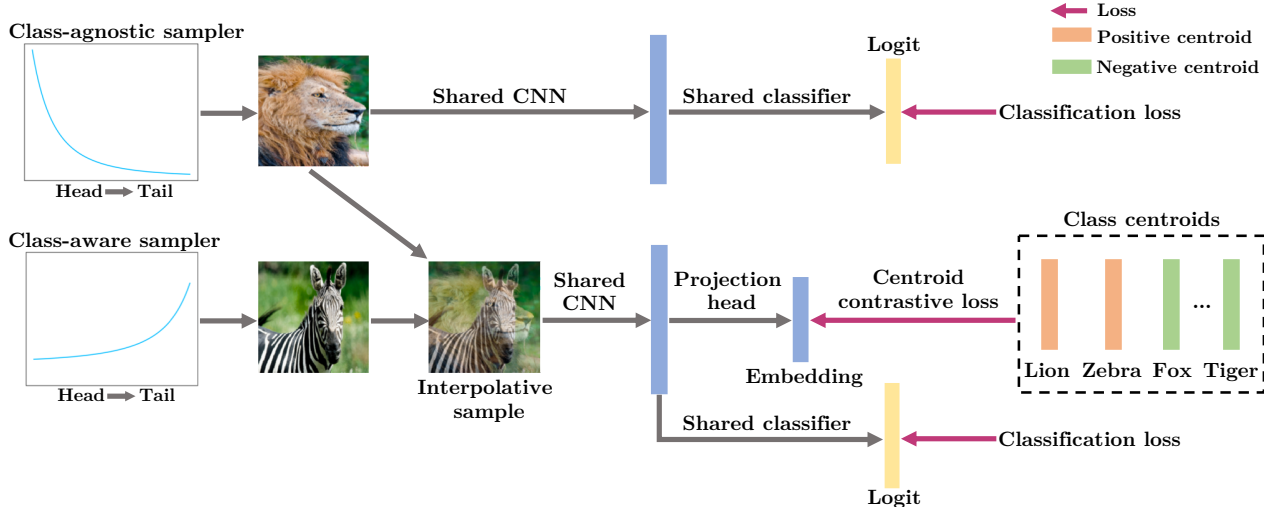


Figure 2: Interpolative centroid contrastive learning framework. The uniform branch (top) focuses more on head-class samples and is trained with the standard cross entropy loss. The interpolative branch (bottom) focuses more on tail-class samples and is trained with an interpolative classification loss and an interpolative centroid contrastive loss. The model parameters are shared between the two branches.

prototypes and encourages embeddings to gather around their corresponding prototypes. MoPro [28] extends this idea to weakly-supervised learning and calculates prototypes based on exponential moving average.

Different from existing contrastive learning methods, our ICCL operates on an interpolative sample consisting information of both classes returned by the class-agnostic and class-aware sampler. Our contrastive loss seeks to learn a representation for the interpolative sample, such that it can be used to retrieve the centroids for both source classes. The centroid retrieval is performed via non-parametric contrastive similarity matching in the low-dimensional space, thus it is different from Mixup [57] which operates on the parametric classifier.

Mixup. As an effective data augmentation technique, Mixup [57] regularises the neural network by performing convex combination of training samples. Chou *et al.* [6] proposed larger mixing weight for tail classes to push the decision boundary towards the head classes. Several works have applied Mixup to improve contrastive learning representation in *self-supervised* setting [21, 25, 43, 60, 49, 27]. In contrast, our interpolative centroid contrastive loss is a new loss designed to improve *supervised* representation learning under long-tailed distribution.

3. Method

Formally speaking, for a long-tailed classification task, we are given a training dataset $\mathcal{D} = \{(\mathbf{x}_i, y_i)\}_{i=1}^n$, where \mathbf{x}_i is an image and $y_i \in \{1, \dots, K\}$ is its class label. The training dataset can be decomposed into $\mathcal{D} = \mathcal{D}^h \cup \mathcal{D}^t$, where $\mathcal{D}^h = \{(\mathbf{x}_i^h, y_i^h)\}_{i=1}^{n^h}$ comprises of head-class samples and $\mathcal{D}^t = \{(\mathbf{x}_i^t, y_i^t)\}_{i=1}^{n^t}$ consists of tail-class samples. Since

$n^h \gg n^t$, the model needs to learn strong discriminative representations for tail classes in a low-resource and imbalanced setting, such that it is not overwhelmed by the abundant head-class samples and is able to classify both head and tail classes correctly.

3.1. Overall framework

Our proposed long-tailed representation learning framework consists of a uniform and an interpolative branch as illustrated in Figure 2. The uniform branch follows the original long-tailed distribution to learn more generalisable representations from data-rich head-class samples, whereas the interpolative branch focuses more on modelling the tail-class to improve tail-class representation. Both branches share the same model parameters, which is different from BBN [59]. Next, we introduce the components of our framework:

- A convolutional neural network (CNN) encoder which transforms an image into a feature vector $\mathbf{g}_i \in \mathbb{R}^{d_g}$. We experiment with the ResNet [17] model and its variants [55]. The feature \mathbf{g}_i is the output from the global average pooling layer.
- A projection head which transforms the feature vector \mathbf{g}_i into a low-dimensional normalised embedding $\mathbf{z}_i \in \mathbb{R}^{d_z}$. Following SimCLR [4], the projection head is a MLP with one hidden layer of size d_g and ReLU activations.
- A linear classifier with softmax activation which returns a class probability \mathbf{p}_i given a feature vector \mathbf{g}_i .
- Class centroids $\mathbf{c}^k \in \mathbb{R}^{d_z \times K}$ which resides in the low-dimensional embedding space. Similar to MoPro [28], we compute the centroid of each class as the exponential-

moving-average (EMA) of the low-dimensional embeddings for samples from that class. Specifically, the centroid for class k is updated during training by:

$$\mathbf{c}^k \leftarrow m \cdot \mathbf{c}^k + (1 - m) \sum_{k=1}^K \mathbb{1}_{y_i=k} \cdot \mathbf{z}_i, \quad (1)$$

where m is the momentum coefficient.

- A class-agnostic and a class-aware sampler which create interpolative samples.

3.2. Interpolative sample generation

We utilise two different samplers for interpolative sample generation:

- A class-agnostic sampler which selects all samples with an equal probability regardless of the class, thus it returns more head-class samples. We denote a sample returned by the class-agnostic sampler as (\mathbf{x}_i^h, y_i^h) .
- A class-aware sampler which focuses more on tail classes. It first samples a class and then select the corresponding samples uniformly with repetition. Let n^k denotes the number of samples in class k , the probability $p(k)$ of sampling class k is inversely proportional to n^k as follows:

$$p(k) = \frac{(1/n^k)^\gamma}{\sum_{j=1}^K (1/n^j)^\gamma}, \quad (2)$$

where γ is an adjustment parameter. When $\gamma = 0$, the class-aware sampler is equivalent to the balanced sampler in [42]. When $\gamma = 1$, it is the reverse sampler in [59]. We denote a sample returned by the class-aware sampler as (\mathbf{x}_i^t, y_i^t) .

An interpolative image \mathbf{x}_i^f is formed by linearly combining two images from the class-agnostic and class-aware sampler, respectively.

$$\mathbf{x}_i^f = \lambda \mathbf{x}_i^h + (1 - \lambda) \mathbf{x}_i^t, \quad (3)$$

where $\lambda \sim \mathcal{U}(0, 1)$ is sampled from a uniform distribution. It is equivalent to the Beta(α, α) used in Mixup [57] with $\alpha = 1$. Our contrastive learning trains the model such that the representation of the interpolative image is discriminative for both class y_i^h and class y_i^t .

3.3. Interpolative centroid contrastive loss

Here we introduce the proposed interpolative centroid contrastive loss which aims to improve long-tailed representation learning. Given the low-dimensional embedding \mathbf{z}_i^f for an interpolative sample \mathbf{x}_i^f , we use \mathbf{z}_i^f to query the class centroids with contrastive similarity matching. Specifically,

the probability that the k -th class centroid \mathbf{c}^k is retrieved is given as:

$$p(\mathbf{c}^k | \mathbf{x}_i^f) = \frac{\exp(\mathbf{z}_i^f \cdot \mathbf{c}^k / \tau)}{\sum_{j=1}^K \exp(\mathbf{z}_i^f \cdot \mathbf{c}^j / \tau)}, \quad (4)$$

where τ is a scalar temperature parameter to scale the similarity. Equation 4 can be interpreted as a non-parametric classifier. Since the centroid is computed as the moving-average of \mathbf{z}_i , it does not suffer from the problem of weight imbalance as a parametric classifier does.

Since \mathbf{x}_i^f is a linear interpolation of \mathbf{x}_i^h and \mathbf{x}_i^t (see equation 3), our loss encourages the retrieval of the corresponding centroids of class y_i^h and y_i^t . Thus, the interpolative centroid contrastive loss is defined as:

$$\mathcal{L}_{cc}^{it} = -\lambda \log(p(\mathbf{c}^{y_i^h} | \mathbf{x}_i^f)) - (1 - \lambda) \log(p(\mathbf{c}^{y_i^t} | \mathbf{x}_i^f)). \quad (5)$$

The proposed centroid contrastive loss introduces valuable structural information into the embedding space. The numerator of $p(\mathbf{c} | \mathbf{x}_i^f)$ reduces the intra-class variance by pulling embeddings with the same class closer to the class centroid. The denominator of $p(\mathbf{c} | \mathbf{x}_i^f)$ increases the inter-class variance by pushing an embedding away from other classes' centroids. Therefore, more discriminative representations can be learned.

3.4. Classification loss

Given the classifier's output prediction probability $p(\mathbf{x}_i^h)$ for an image \mathbf{x}_i^h , we define the classification loss on the uniform branch as the standard cross entropy loss:

$$\mathcal{L}_{ce} = -\log(p^{y_i^h}(\mathbf{x}_i^h)). \quad (6)$$

For an interpolative sample \mathbf{x}_i^f from the interpolative branch, the classification loss is

$$\mathcal{L}_{ce}^{it} = -\lambda \log(p^{y_i^h}(\mathbf{x}_i^f)) - (1 - \lambda) \log(p^{y_i^t}(\mathbf{x}_i^f)). \quad (7)$$

3.5. Overall loss

During training, we jointly minimise the sum of losses on both branches:

$$\mathcal{L}_{total} = \sum_{i=1}^n \omega_u \mathcal{L}_{ce} + \omega_{it} (\mathcal{L}_{ce}^{it} + \mathcal{L}_{cc}^{it}), \quad (8)$$

where ω_u and ω_{it} are the weights for the uniform branch and the interpolative branch, respectively.

3.6. Classifier rebalancing

Following the decoupled training approach [22], we rebalance our classifier after the representation learning stage. Specifically, we discard the projection head and fine-tune

Dataset Imbalance ratio	Long-tailed CIFAR100			Long-tailed CIFAR10		
	100	50	10	100	50	10
CE*	38.3	43.9	55.7	70.4	74.8	86.4
Focal Loss* [30]	38.4	44.3	55.8	70.4	76.7	86.7
Mixup* [57]	39.5	45.0	58.0	73.1	77.8	87.1
Manifold Mixup* [48]	38.3	43.1	56.6	73.0	78.0	87.0
Manifold Mixup (two samplers)* [48]	36.8	42.1	56.5	73.1	79.2	86.8
CB-Focal* [8]	39.6	45.2	58.0	74.6	79.3	87.1
CE-DRW* [1]	41.5	45.3	58.1	76.3	80.0	87.6
CE-DRS* [1]	41.6	45.5	58.1	75.6	79.8	87.4
LDAM-DRW* [1]	42.0	46.6	58.7	77.0	81.0	88.2
cRT [†] [22]	42.3	46.8	58.1	75.7	80.4	88.3
LWS [†] [22]	42.3	46.4	58.1	73.0	78.5	87.7
BBN [59]	42.6	47.0	59.1	79.8	82.2	88.3
M2m [24]	43.5	-	57.6	79.1	-	87.5
De-confound-TDE [45]	44.1	50.3	59.6	80.6	83.6	88.5
ICCL (ours)	46.6	51.6	62.1	82.1	84.7	89.7

Table 1: Top-1 accuracy on CIFAR100-LT and CIFAR10-LT with different imbalance ratios using ResNet-32 CIFAR. Here, * denotes results copied from Zhou *et al.* [59]. [†] denotes our reproduced results based on Kang *et al.* [22] setting.

the linear classifier. The CNN encoder is either fixed or fine-tuned with a smaller learning rate. In order to rebalance the classifier towards tail classes, we employ our class-aware sampler. We denote the sampler’s adjustment parameter as γ' . Due to more frequent sampling of tail-class samples by the class-aware sampler, the classifier’s logits distribution would shift towards the tail classes at the cost of lower accuracy on head classes. In order to maintain the head-class accuracy, we introduce a distillation loss [18, 46] using the classifier from the first stage as the teacher. The overall loss for classifier rebalancing consists of a cross-entropy classification loss and a KL-divergence distillation loss.

$$\mathcal{L}_{cb} = \sum_{i=1}^n (1 - \omega_d) \mathcal{L}_{ce} + \omega_d \tau_d^2 \mathcal{L}_{KL}(\sigma(\mathbf{o}^T / \tau_d), \sigma(\mathbf{o}^S / \tau_d)), \quad (9)$$

where ω_d is the weight of the distillation loss, \mathbf{o}^S and \mathbf{o}^T are the class logits produced by the student classifier (2nd stage) and the teacher classifier (1st stage), respectively. τ_d is the distillation temperature and σ is the softmax function.

For inference, we use a classification network consisting of the CNN encoder followed by the rebalanced classifier.

4. Experiments

4.1. Dataset

We evaluate our method on three standard benchmark datasets for long-tail recognition as follows:

CIFAR-LT. CIFAR10-LT and CIFAR100-LT contain samples from the CIFAR10 and CIFAR100 [26] dataset, respectively. The class sampling frequency follows an exponential distribution. Following [59, 1], we construct LT datasets with different imbalance ratios of 100, 50, and 10. Imbalance ratio is defined as the ratio of maximum to the

minimum class sampling frequency. The number of training images for CIFAR10-LT with an imbalance ratio of 100, 50 and 10 is 12k, 14k and 20k, respectively. Similarly, CIFAR100-LT has a training set size of 11k, 13k and 20k. Both test sets are balanced with the original size of 10k.

ImageNet-LT. The training set consists of 1000 classes with 116k images sampled from the ImageNet [10] dataset. The class sampling frequency follows a Pareto distribution with a shape parameter of 6 [36]. The imbalance ratio is 256. Despite a smaller training size, it retains ImageNet [10] original test set size of 50k.

iNaturalist 2018. It is a real-world long-tailed dataset for fine-grained image classification of 8,142 species [47]. We utilise the official training and test datasets composing of 438k training and 24k test images.

4.2. Evaluation

For all datasets, we evaluate our models on the test sets and report the overall top-1 accuracy across all classes. To further access the model’s accuracy on different classes, we group the classes into splits according to their number of images [36, 22]: many (> 100 images), medium (20 – 100 images) and few (< 20 images).

4.3. Implementation details

For fair comparison, we follow the same training setup of previous works using SGD optimiser with a momentum of 0.9. For all experiments, we fix class centroid momentum coefficient $m = 0.99$, class-aware sampler adjustment parameter $\gamma = 0$, $\gamma' = 1$, distillation weight $\omega_d = 0.5$ and distillation temperature $\tau_d = 10$. Unless otherwise specified, for the hyperparameters, we set temperature $\tau = 0.07$, uniform branch weight $\omega_u = 1$, interpolative

Method	Overall	Many	Medium	Few
OLTR* [36]	41.9	51.0	40.8	20.8
Focal Loss* [30]	43.7	64.3	37.1	8.2
NCM [22]	47.3	56.6	45.3	28.1
τ -norm [22]	49.4	59.1	46.9	30.7
cRT [22]	49.6	61.8	46.2	27.4
LWS [22]	49.9	60.2	47.2	30.3
De-confound-TDE [45]	51.8	62.7	48.8	31.6
cRT [†] [22]	52.4	64.3	49.1	30.7
LWS [†] [22]	52.5	63.0	49.6	32.8
De-confound-TDE [†] [45]	52.4	63.5	49.2	32.2
ICCL (ours)	54.0	60.7	52.9	39.0

Table 2: Top-1 accuracy on ImageNet-LT using ResNeXt-50. * denotes results copied from Tang *et al.* [45]. † denotes our reproduced results using improved settings. The trade-off between head class (i.e. many) and tail class (i.e. medium and few) accuracy is adjustable without affecting the overall accuracy (see Fig. 4).

branch weight $\omega_{it} = 1$, and MLP projection head embedding size $d_z = 128$ in the representation learning stage. In the classifier balancing stage, we freeze the CNN and fine-tune the classifier using the original learning rate $\times 0.1$ with cosine scheduling [37] for 10 epochs.

We also design a warm-up training curriculum. Specifically, In the first T epochs, we train only the uniform branch using the cross-entropy loss \mathcal{L}_{ce} and a (non-interpolative) centroid contrastive loss $\mathcal{L}_{cc} = -\log(p(\mathbf{c}^{y_i^h} | \mathbf{x}_i^h))$. After T epochs, we activate the interpolative branch and optimise \mathcal{L}_{total} in Equation 8. The warm-up provides good initialisation for the representations and the centroids. T is scheduled to be approximately halfway through the total number of epochs.

CIFAR-LT. We use a ResNet-32 [17] as the CNN encoder and follow the training strategies in [59]. We train the model for 200 epochs with a batch size of 128. The projected embedding size is $d_z = 32$. We use standard data augmentation which consists of random horizontal flip and cropping with a padding size of 4. The learning rate warms up to 0.1 within the first 5 epochs and decays at epoch 120 and 160 with a step size of 0.01. We use a weight decay of $2e-4$. We set $\tau = 0.3$ and T as 80 and 100 epochs for CIFAR100-LT and CIFAR10-LT, respectively. ω_u is set as 0 after warm-up. In the classifier balancing stage, we fine-tune the CNN encoder using cosine scheduling with an initial learning rate of 0.01.

ImageNet-LT. We train a ResNeXt-50 [55] model for 90 epochs using a batch size of 256, a weight decay of $5e-4$, and a base learning rate of 0.1 with cosine scheduling. Similar to [22], we augment the data using random horizontal flip, cropping and colour jittering. We set $T = 40$.

iNaturalist 2018. Following [22], we train a ResNet-50 model for 90 epochs and 200 epochs using 0.2 learning rate with cosine decay, 512 batch size and $1e-4$ weight decay. The data augmentation comprises of only horizontal flip and cropping. T is set as 40 and 100 epochs for training epochs

of 90 and 200, respectively.

4.4. Results

Next we present the results, where the proposed ICCL achieves significant improved performance on all benchmarks.

CIFAR-LT. Table 1 demonstrates that ICCL surpasses existing methods across different imbalance ratios for both CIFAR100-LT and CIFAR10-LT. Notably, after the representation learning stage, our approach generally achieves competitive performance compared to existing methods apart from De-confound-TDE [45]. By balancing the classifier, the performance of ICCL further improves and outperforms De-confound-TDE by 2.5% on the more challenging CIFAR100-LT with imbalance ratio of 100.

ImageNet-LT. Table 2 presents the ImageNet-LT results, where ICCL outperforms the existing methods. For ImageNet-LT, we also propose an improved set of hyperparameters which increases the accuracy for existing methods. Specifically, different from the original hyperparameters used in [22], we use a smaller batch size of 256 and a learning rate of 0.1. Furthermore, we find it is better to use original learning rate $\times 0.1$ for classifier balancing. For fair comparison, we re-implement Decouple methods [22] and De-confound-TDE [45] using our settings and obtain better accuracy than those reported in the original papers. However, ICCL still achieves the best overall accuracy of 54.0% with noticeable accuracy gains on medium and few classes.

iNaturalist 2018. On the real-world large-scale iNaturalist 2018 dataset, ICCL achieves substantial improvements compared with existing methods as shown in Table 3. For 90 and 200 epochs, our method surpasses BBN [59] by 4.1% and 2.8% respectively. We obtain the split accuracy of BBN based on the checkpoint released by the authors. We observe that BBN suffers from a large discrepancy of 21.4% between the many and medium class accuracy for 90 epochs, whereas our method has more consistent accuracy

Method	90 Epochs				200 Epochs			
	Overall	Many	Medium	Few	Overall	Many	Medium	Few
CB-Focal [8]	61.1	-	-	-	-	-	-	-
CE-DRS* [1]	63.6	-	-	-	-	-	-	-
CE-DRW* [1]	63.7	-	-	-	-	-	-	-
LDAM-DRW [1]	68.0	-	-	-	-	-	-	-
LDAM-DRW* [1]	64.6	-	-	-	66.1	-	-	-
NCM [22]	58.2	55.5	57.9	59.3	63.1	61.0	63.5	63.3
cRT [22]	65.2	69.0	66.0	63.2	68.2	73.2	68.8	66.1
τ -norm [22]	65.6	65.6	65.3	65.9	69.3	71.1	68.9	69.3
LWS [22]	65.9	65.0	66.3	65.5	69.5	71.0	69.8	68.8
BBN [59]	66.4	49.4	70.8	65.3	69.7	61.7	73.6	66.9
ICCL (ours)	70.5	67.6	70.2	71.6	72.5	72.1	72.3	72.9

Table 3: Top-1 accuracy on iNaturalist 2018 using ResNet-50 for 90 epochs and 200 epochs. * denotes results copied from Zhou *et al.* [59] which uses 90 and 180 epochs. The trade-off between head class (i.e. many) and tail class (i.e. medium and few) is adjustable without affecting the overall accuracy (see Fig. 4).

\mathcal{L}_{ce}	\mathcal{L}_{ce}^{it}	\mathcal{L}_{cc}^{it}	Warm-up	Overall	Head	Tail
✓				51.3	60.6	45.5
	✓			51.6	58.3	47.4
	✓		✓	51.7	57.9	47.9
✓		✓	✓	52.4	59.9	47.7
✓	✓		✓	53.4	61.1	48.6
✓	✓	✓		53.6	61.2	48.8
✓	✓	✓	✓	54.0	60.7	49.8

Table 4: Ablation study on different components of ICCL on ImageNet-LT. Head denotes the many split, whereas tail includes the medium and few splits. The proposed \mathcal{L}_{ce}^{it} , \mathcal{L}_{cc}^{it} , and warm-up all contribute to accuracy improvement. Using only \mathcal{L}_{ce}^{it} is equivalent to Mixup [57].

Beta(α, β)	CIFAR100-LT
(0.2, 1.0)	43.6
(0.2, 0.2)	43.8
(0.6, 0.6)	45.4
(1.0, 1.0)	46.6
(2.0, 2.0)	46.8

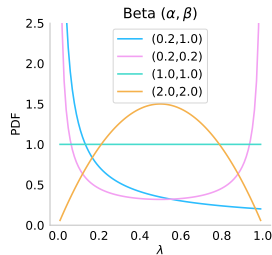


Table 5: Effect of sampling λ from different Beta(α, β) on CIFAR100-LT. λ determines the weighting of the two samples for a given interpolative sample.

across all splits. Additionally, ICCL obtains a best overall accuracy of 70.5% at 90 epochs which is better than BBN (69.7%) at 180 epochs.

4.5. Ablation study

Here we perform extensive ablation study to examine the effect of each component and hyperparameters of ICCL, and provide analysis on what makes ICCL successful.

Loss components. For representation learning, ICCL introduces the interpolative centroid contrastive loss \mathcal{L}_{cc}^{it} and the interpolative cross-entropy loss \mathcal{L}_{ce}^{it} as shown in Equa-

Sampler	CIFAR100-LT	CIFAR10-LT	ImageNet-LT	iNaturalist
Uniform	44.7	79.9	52.8	69.4
$\gamma = 0$	46.6	82.1	54.0	70.5
$\gamma = 0.5$	46.2	81.6	54.1	70.2
$\gamma = 1.0$	46.2	81.1	53.1	70.1

Table 6: Adjustment parameter γ of the interpolative branch class-aware sampler. Focus excessively on head-class (uniform) or tail-class samples ($\gamma = 1$) leads to worse performance.

tion 8. In Table 4, we evaluate the contribution of each loss components using ImageNet-LT dataset. We consider many split as the head classes (> 100 images per class), medium and few splits as the tail classes (≤ 100 images per class). We employ the same classifier balancing technique as described in Section 3.4. We observe that both \mathcal{L}_{ce}^{it} and \mathcal{L}_{cc}^{it} improve the overall accuracy individually and collectively. By comparing with \mathcal{L}_{ce}^{it} only which is equivalent to Mixup [57], we demonstrate that our loss formulation achieves superior performance. Additionally, having a warm-up before incorporating interpolative losses provides an extra accuracy boost, especially for the tail classes. This aligns with the observation in [1] which suggests that adopting a deferred schedule before re-sampling is better for representation learning.

Interpolation weight λ . In Equation 3, We sample the interpolation weight $\lambda \in [0, 1]$ from a uniform distribution, which is equivalent to Beta(1, 1). We vary the beta distribution and study its effect on CIFAR100-LT with an imbalance ratio of 100. The resulting accuracy and the corresponding beta distribution are shown in Table 5. Sampling from Beta(0.2, 1.0) is more likely to return a small λ , thus the interpolative samples contain more information about images from the class-aware sampler. As we fix $\alpha = \beta$ and increase them from 0.2 to 2, the accuracy increases. Good performance can be achieved with Beta(1.0, 1.0) and Beta(2.0, 2.0), where the sampled λ is less likely to be an extreme value.

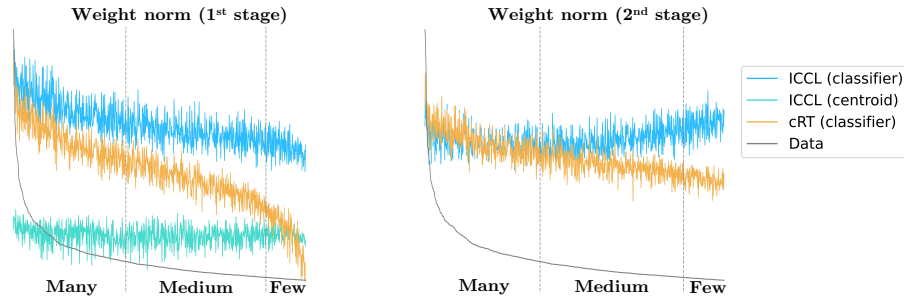


Figure 3: Visualisation of classifier’s weight norm and centroid’s norm of ICCL after the representation learning (left) and classifier balancing stage (right) on ImageNet-LT. Comparing with cRT [22], the weight norm of our ICCL classifier is more balanced. Additionally, the class centroids have intrinsically balanced norm.

Method	Rebalancing	Overall	Many	Medium	Few
CE [22]	-	46.7	68.1	40.2	9.0
ICCL (ours)	-	50.5	68.5	44.4	20.8
CE [22]	✓	52.4	64.3	49.1	30.7
ICCL (ours)	✓	54.0	60.7	52.9	39.0

Table 7: Effect of classifier rebalancing on ImageNet-LT. ICCL learns better tail-class representation which leads to higher tail-class (i.e. medium and few) accuracy after classifier rebalancing.

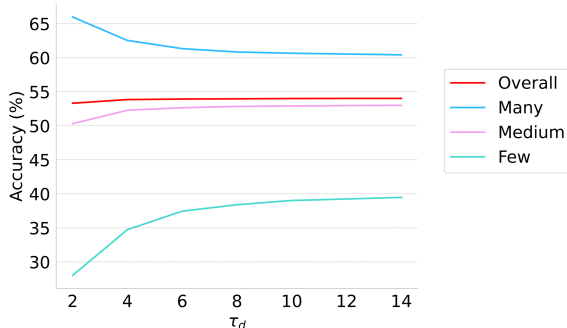


Figure 4: Effect of distillation temperature τ_d on ImageNet-LT. ICCL’s overall accuracy is not sensitive to τ_d variation.

Class-aware sampler adjustment parameter γ . We further investigate the influence of γ on representation learning. When $\gamma = 0$ and 1, the class-aware sampler is equivalent to class-balanced sampler [42] and reverse sampler [59] respectively. We include a class-agnostic uniform sampler as the baseline. Table 6 shows that the interpolative branch sampler should neither focus excessively on the tail classes ($\gamma = 1$) nor on the head classes (uniform). When using either of these two samplers, the resulting interpolative image might be less informative due to excessive repetition of tail-class samples or redundant head-class samples.

Rebalancing classifier. In Table 7, we show the effect of classifier rebalancing, which improves both ICCL and the baseline CE method [22]. By learning better tail-class representation, ICCL achieves higher overall accuracy compared to [22] both before and after classifier rebalancing.

Classifier balancing parameters. In the classifier bal-

γ'	ω_d	CIFAR100-LT	CIFAR10-LT	iNaturalist	ImageNet-LT	
		ICCL	ICCL	ICCL	ICCL	cRT [22]
0	0	45.3	77.5	69.5	53.7	52.4
0	0.5	45.0	77.6	69.5	53.2	52.2
1	0	47.1	82.3	70.2	53.6	49.6
1	0.5	46.6	82.1	70.5	54.0	51.3

Table 8: Ablation study for classifier balancing methods. ICCL benefits from using a reverse sampler ($\gamma' = 1$) and knowledge distillation ($\omega_d = 0.5$), especially for the more complex ImageNet-LT and iNaturalist datasets.

ancing stage, we fix the sampler adjustment parameter $\gamma' = 1$, and the distillation weight $\omega_d = 0.5$. We study their effects in Table 8. For our ICCL approach, using a reverse sampler ($\gamma' = 1$) is better than a balanced sampler ($\gamma' = 0$). Furthermore, the distillation loss tends to benefit more complex ImageNet-LT and iNaturalist than CIFAR-LT datasets. For the baseline cRT [22], applying the reverse sampler and distillation does not give accuracy improvement compared to the default setting (52.4).

Weight norm visualisation. The L_2 norms of the weights for the linear classification layer suggest how balanced the classifier is. Having a high weight norm for a particular class indicates that the classifier is more likely to generate a high logit score for that class. Figure 3 depicts the weight norm of ICCL and cRT [22] after the representation learning and classifier balancing stage. In both stages, our ICCL classifier has a more balanced weight norm compared with cRT. Furthermore, we also plot the norm of our class centroids e^k , which shows that the centroids are intrinsically balanced across different classes.

Distillation temperature τ_d . In Figure 4, we study how τ_d affects the accuracy of ICCL on ImageNet-LT. We find that the overall accuracy is not sensitive to changes in τ_d . As τ_d increases, the teacher’s logit distribution becomes more flattened. Therefore, the accuracy for medium and few class improves, whereas the accuracy for many class decreases.

5. Conclusion

In this work, we propose an interpolative centroid contrastive learning technique for long-tailed representation learning. By utilising class centroids and interpolative losses, we strengthen the discriminative power of the learned representations, leading to improved classification accuracy. We demonstrate the effectiveness of our approach with significant improvement on multiple long-tailed classification benchmarks.

6. Acknowledgments

Anthony Meng Huat Tiong is supported by Salesforce and the Singapore Economic Development Board under the Industrial Postgraduate Programme. Boyang Li is supported by the Nanyang Associate Professorship and the National Research Foundation Fellowship (NRF-NRFF13-2021-0006), Singapore. Any opinions, findings, conclusions, or recommendations expressed in this material are those of the authors and do not reflect the views of the funding agencies.

References

- [1] Kaidi Cao, Colin Wei, Adrien Gaidon, Nikos Arachiga, and Tengyu Ma. Learning imbalanced datasets with label-distribution-aware margin loss. In *NeurIPS*, pages 1567–1578, 2019.
- [2] Nitesh V Chawla, Kevin W Bowyer, Lawrence O Hall, and W Philip Kegelmeyer. Smote: synthetic minority over-sampling technique. *Journal of artificial intelligence research*, 16:321–357, 2002.
- [3] Nitesh V Chawla, Aleksandar Lazarevic, Lawrence O Hall, and Kevin W Bowyer. Smoteboost: Improving prediction of the minority class in boosting. In *European conference on principles of data mining and knowledge discovery*, pages 107–119. Springer, 2003.
- [4] Ting Chen, Simon Kornblith, Mohammad Norouzi, and Geoffrey Hinton. A simple framework for contrastive learning of visual representations. In *ICML*, 2020.
- [5] Xinlei Chen, Haoqi Fan, Ross Girshick, and Kaiming He. Improved baselines with momentum contrastive learning. *arXiv preprint arXiv:2003.04297*, 2020.
- [6] Hsin-Ping Chou, Shih-Chieh Chang, Jia-Yu Pan, Wei Wei, and Da-Cheng Juan. Remix: Rebalanced mixup. In *ECCV*, pages 95–110. Springer, 2020.
- [7] Peng Chu, Xiao Bian, Shaopeng Liu, and Haibin Ling. Feature space augmentation for long-tailed data. In *ECCV*, 2020.
- [8] Yin Cui, Menglin Jia, Tsung-Yi Lin, Yang Song, and Serge Belongie. Class-balanced loss based on effective number of samples. In *CVPR*, pages 9268–9277, 2019.
- [9] Yin Cui, Yang Song, Chen Sun, Andrew Howard, and Serge Belongie. Large scale fine-grained categorization and domain-specific transfer learning. In *CVPR*, pages 4109–4118, 2018.
- [10] Jia Deng, Wei Dong, Richard Socher, Li-Jia Li, Kai Li, and Fei-Fei Li. Imagenet: A large-scale hierarchical image database. In *CVPR*, pages 248–255, 2009.
- [11] Jiankang Deng, Jia Guo, Niannan Xue, and Stefanos Zafeiriou. Arcface: Additive angular margin loss for deep face recognition. In *CVPR*, pages 4690–4699, 2019.
- [12] Qi Dong, Shaogang Gong, and Xiatian Zhu. Class rectification hard mining for imbalanced deep learning. In *ICCV*, pages 1851–1860, 2017.
- [13] Chris Drummond, Robert C Holte, et al. C4. 5, class imbalance, and cost sensitivity: why under-sampling beats over-sampling. In *Workshop on learning from imbalanced datasets II*, volume 11, pages 1–8. Citeseer, 2003.
- [14] Jean-Bastien Grill, Florian Strub, Florent Altché, Corentin Tallec, Pierre H. Richemond, Elena Buchatskaya, Carl Doersch, Bernardo Avila Pires, Zhaohan Daniel Guo, Mohammad Gheshlaghi Azar, Bilal Piot, Koray Kavukcuoglu, Rémi Munos, and Michal Valko. Bootstrap your own latent: A new approach to self-supervised learning. *arXiv preprint arXiv:2006.07733*, 2020.
- [15] Hui Han, Wen-Yuan Wang, and Bing-Huan Mao. Borderline-smote: a new over-sampling method in imbalanced data sets learning. In *International conference on intelligent computing*, pages 878–887. Springer, 2005.
- [16] Kaiming He, Haoqi Fan, Yuxin Wu, Saining Xie, and Ross Girshick. Momentum contrast for unsupervised visual representation learning. In *Proceedings of the IEEE/CVF Conference on Computer Vision and Pattern Recognition*, pages 9729–9738, 2020.
- [17] Kaiming He, Xiangyu Zhang, Shaoqing Ren, and Jian Sun. Deep residual learning for image recognition. In *CVPR*, pages 770–778, 2016.
- [18] Geoffrey Hinton, Oriol Vinyals, and Jeff Dean. Distilling the knowledge in a neural network. *arXiv preprint arXiv:1503.02531*, 2015.
- [19] Chen Huang, Yining Li, Chen Change Loy, and Xiaoou Tang. Learning deep representation for imbalanced classification. In *CVPR*, pages 5375–5384, 2016.
- [20] Muhammad Abdullah Jamal, Matthew Brown, Ming-Hsuan Yang, Liqiang Wang, and Boqing Gong. Rethinking class-balanced methods for long-tailed visual recognition from a domain adaptation perspective. In *CVPR*, pages 7610–7619, 2020.
- [21] Yannis Kalantidis, Mert Bulent Sariyildiz, Noe Pion, Philippe Weinzaepfel, and Diane Larlus. Hard negative mixing for contrastive learning. In *NeurIPS*, 2020.
- [22] Bingyi Kang, Saining Xie, Marcus Rohrbach, Zhicheng Yan, Albert Gordo, Jiashi Feng, and Yannis Kalantidis. Decoupling representation and classifier for long-tailed recognition. In *ICLR*, 2020.
- [23] Salman H Khan, Munawar Hayat, Mohammed Bennamoun, Ferdous A Sohel, and Roberto Togneri. Cost-sensitive learning of deep feature representations from imbalanced data. *IEEE transactions on neural networks and learning systems*, 29(8):3573–3587, 2017.
- [24] Jaehyung Kim, Jongheon Jeong, and Jinwoo Shin. M2m: Imbalanced classification via major-to-minor translation. In

- Proceedings of the IEEE/CVF Conference on Computer Vision and Pattern Recognition*, pages 13896–13905, 2020.
- [25] Sungnyun Kim, Gihun Lee, Sangmin Bae, and Se-Young Yun. Mixco: Mix-up contrastive learning for visual representation. In *NeurIPS Workshop*, 2020.
- [26] Alex Krizhevsky and Geoffrey Hinton. Learning multiple layers of features from tiny images. Technical report, 2009.
- [27] Kibok Lee, Yian Zhu, Kihyuk Sohn, Chun-Liang Li, Jinwoo Shin, and Honglak Lee. i-mix: A domain-agnostic strategy for contrastive representation learning. In *ICLR*, 2021.
- [28] Junnan Li, Caiming Xiong, and Steven CH Hoi. Mopro: Webly supervised learning with momentum prototypes. *arXiv preprint arXiv:2009.07995*, 2020.
- [29] Junnan Li, Pan Zhou, Caiming Xiong, Richard Socher, and Steven C.H. Hoi. Prototypical contrastive learning of unsupervised representations. *arXiv preprint arXiv:2005.04966*, 2020.
- [30] Tsung-Yi Lin, Priya Goyal, Ross Girshick, Kaiming He, and Piotr Dollár. Focal loss for dense object detection. In *ICCV*, pages 2980–2988, 2017.
- [31] Tsung-Yi Lin, Michael Maire, Serge Belongie, James Hays, Pietro Perona, Deva Ramanan, Piotr Dollár, and C Lawrence Zitnick. Microsoft coco: Common objects in context. In *ECCV*, pages 740–755. Springer, 2014.
- [32] Jialun Liu, Yifan Sun, Chuchu Han, Zhaopeng Dou, and Wenhui Li. Deep representation learning on long-tailed data: A learnable embedding augmentation perspective. In *CVPR*, pages 2970–2979, 2020.
- [33] Weiyang Liu, Yandong Wen, Zhiding Yu, Ming Li, Bhiksha Raj, and Le Song. Sphereface: Deep hypersphere embedding for face recognition. In *CVPR*, pages 212–220, 2017.
- [34] Weiyang Liu, Yandong Wen, Zhiding Yu, and Meng Yang. Large-margin softmax loss for convolutional neural networks. In *ICML*, volume 2, page 7, 2016.
- [35] Xu-Ying Liu, Jianxin Wu, and Zhi-Hua Zhou. Exploratory undersampling for class-imbalance learning. *IEEE Transactions on Systems, Man, and Cybernetics, Part B (Cybernetics)*, 39(2):539–550, 2008.
- [36] Ziwei Liu, Zhongqi Miao, Xiaohang Zhan, Jiayun Wang, Boqing Gong, and Stella X. Yu. Large-scale long-tailed recognition in an open world. In *CVPR*, pages 2537–2546, 2019.
- [37] Ilya Loshchilov and Frank Hutter. Sgdr: Stochastic gradient descent with warm restarts. *arXiv preprint arXiv:1608.03983*, 2016.
- [38] Dhruv Mahajan, Ross Girshick, Vignesh Ramanathan, Kaiming He, Manohar Paluri, Yixuan Li, Ashwin Bharambe, and Laurens van der Maaten. Exploring the limits of weakly supervised pretraining. In *ECCV*, pages 181–196, 2018.
- [39] Aditya Krishna Menon, Sadeep Jayasumana, Ankit Singh Rawat, Himanshu Jain, Andreas Veit, and Sanjiv Kumar. Long-tail learning via logit adjustment. *ICLR*, 2021.
- [40] Tomas Mikolov, Ilya Sutskever, Kai Chen, Greg S Corrado, and Jeff Dean. Distributed representations of words and phrases and their compositionality. In *NeurIPS*, pages 3111–3119, 2013.
- [41] David MW Powers. Applications and explanations of zipf’s law. In *New methods in language processing and computational natural language learning*, 1998.
- [42] Li Shen, Zhouchen Lin, and Qingming Huang. Relay back-propagation for effective learning of deep convolutional neural networks. In *ECCV*, pages 467–482. Springer, 2016.
- [43] Zhiqiang Shen, Zechun Liu, Zhuang Liu, Marios Savvides, Trevor Darrell, and Eric Xing. Un-mix: Rethinking image mixtures for unsupervised visual representation learning. *arXiv preprint arXiv:2003.05438*, 2020.
- [44] Jun Shu, Qi Xie, Lixuan Yi, Qian Zhao, Sanping Zhou, Zongben Xu, and Deyu Meng. Meta-weight-net: Learning an explicit mapping for sample weighting. In *NeurIPS*, pages 1919–1930, 2019.
- [45] Kaihua Tang, Jianqiang Huang, and Hanwang Zhang. Long-tailed classification by keeping the good and removing the bad momentum causal effect. In *NeurIPS*, 2020.
- [46] Yonglong Tian, Dilip Krishnan, and Phillip Isola. Contrastive representation distillation. In *ICLR*, 2020.
- [47] Grant Van Horn, Oisín Mac Aodha, Yang Song, Yin Cui, Chen Sun, Alex Shepard, Hartwig Adam, Pietro Perona, and Serge Belongie. The inaturalist species classification and detection dataset. In *CVPR*, pages 8769–8778, 2018.
- [48] Vikas Verma, Alex Lamb, Christopher Beckham, Amir Najafi, Ioannis Mitliagkas, David Lopez-Paz, and Yoshua Bengio. Manifold mixup: Better representations by interpolating hidden states. In *ICML*, pages 6438–6447. PMLR, 2019.
- [49] Vikas Verma, Minh-Thang Luong, Kenji Kawaguchi, Hieu Pham, and Quoc V Le. Towards domain-agnostic contrastive learning. In *ICML*, 2021.
- [50] Hao Wang, Yitong Wang, Zheng Zhou, Xing Ji, Dihong Gong, Jingchao Zhou, Zhifeng Li, and Wei Liu. Cosface: Large margin cosine loss for deep face recognition. In *CVPR*, pages 5265–5274, 2018.
- [51] Xudong Wang, Long Lian, Zhongqi Miao, Ziwei Liu, and Stella X Yu. Long-tailed recognition by routing diverse distribution-aware experts. *ICLR*, 2021.
- [52] Yu-Xiong Wang, Deva Ramanan, and Martial Hebert. Learning to model the tail. In *NeurIPS*, pages 7029–7039, 2017.
- [53] Zhirong Wu, Yuanjun Xiong, Stella X. Yu, and Dahua Lin. Unsupervised feature learning via non-parametric instance discrimination. In *CVPR*, pages 3733–3742, 2018.
- [54] Liuyu Xiang and Guiguang Ding. Learning from multiple experts: Self-paced knowledge distillation for long-tailed classification. In *ECCV*, 2020.
- [55] Saining Xie, Ross Girshick, Piotr Dollár, Zhuowen Tu, and Kaiming He. Aggregated residual transformations for deep neural networks. In *Proceedings of the IEEE conference on computer vision and pattern recognition*, pages 1492–1500, 2017.
- [56] Yuzhe Yang and Zhi Xu. Rethinking the value of labels for improving class-imbalanced learning. In *NeurIPS*, 2020.
- [57] Hongyi Zhang, Moustapha Cisse, Yann N Dauphin, and David Lopez-Paz. mixup: Beyond empirical risk minimization. In *ICLR*, 2018.
- [58] Yaoyao Zhong, Weihong Deng, Mei Wang, Jiani Hu, Jianteng Peng, Xunqiang Tao, and Yaohai Huang. Unequal

- training for deep face recognition with long-tailed noisy data. In *CVPR*, pages 7812–7821, 2019.
- [59] Boyan Zhou, Quan Cui, Xiu-Shen Wei, and Zhao-Min Chen. BBN: Bilateral-branch network with cumulative learning for long-tailed visual recognition. pages 1–8, 2020.
- [60] Hong-Yu Zhou, Shuang Yu, Cheng Bian, Yifan Hu, Kai Ma, and Yefeng Zheng. Comparing to learn: Surpassing imagenet pretraining on radiographs by comparing image representations. In *MICCAI*. Springer, 2020.
- [61] Zhi-Hua Zhou and Xu-Ying Liu. Training cost-sensitive neural networks with methods addressing the class imbalance problem. *IEEE Transactions on knowledge and data engineering*, 18(1):63–77, 2005.
- [62] Linchao Zhu and Yi Yang. Inflated episodic memory with region self-attention for long-tailed visual recognition. In *CVPR*, pages 4344–4353, 2020.